ISSN 0023-1584, Kinetics and Catalysis, 2023, Vol. 64, No. 2, pp. 191–200. © Pleiades Publishing, Ltd., 2023.
Russian Text © The Author(s), 2023, published in Kinetika i Kataliz, 2023, Vol. 64, No. 2, pp. 216–226.

Effect of the Hydride and Carbide Phases of Palladium Nanoparticles on the Vibration Frequencies of Adsorbed Surface Molecules

O. A. Usoltsev[a], *, B. O. Protsenko[a], A. Yu. Pnevskaya[a], A. N. Bulgakov[a], and A. L. Bugaev[a]

[a] *The Smart Materials Research Institute of the Southern Federal University, Rostov-on-Don, 344090 Russia*

**e-mail: oleg-usol@yandex.ru*

Received March 29, 2022; revised October 27, 2022; accepted November 9, 2022

Abstract—Palladium-based materials, including nanoparticles, are widely used in the petrochemical, pharmaceutical, automotive, and other industries. The hydride, carbide, and oxide phases of palladium formed during the hydrogenation or oxidation reactions of hydrocarbons significantly affect the catalytic properties of the catalyst. Based on theoretical calculations performed by the density functional theory (DFT) method, the effect of Pd–Pd interatomic distances and the presence of carbon atoms occupying octahedral voids in the fcc lattice of palladium on the vibrational frequencies of adsorbed hydrocarbons represented by ethylidene is shown. Theoretical research is supported by experimental data of infrared (IR) diffuse reflectance Fourier-transform spectroscopy (DRIFTS) collected *in situ* during the formation of carbide and hydride phases of palladium in commercial Pd/Al_2O_3 nanocatalyst under the influence of ethylene and hydrogen. The proposed approach can be used to develop new methods for IR spectra analysis leading to the quantitative diagnostics of structural changes in palladium during various catalytic reactions in the *in situ* mode.

Keywords: IR, FTIR, DRIFTS, DFT, palladium carbide, palladium hydride

DOI: 10.1134/S0023158423020088

INTRODUCTION

Palladium catalysts, including supported palladium nanoparticles, are widely used in many industrially relevant reactions, such as hydrogenation [1–4], dehydrogenation [5, 6], selective oxidation [2, 7, 8], selective hydrogenation [9, 10], combustion [11–14]. Many works indicate the formation of palladium hydrides, carbides, and oxides in addition to the initial metal phase in the presence of a reactive substrate, which affects the catalytic properties of materials [3, 4, 8, 9, 15–17]. The formation of these phases can be observed both by surface-sensitive methods, for example, X-ray photoelectron spectroscopy (XPS) [4, 18], and by volume-sensitive methods that track the change in the electronic state of palladium directly, for example, X-ray absorption near-edge structure (XANES) spectroscopy [15, 16, 19, 20], or indirectly, through observation of the expansion of the face-centered cubic (fcc) lattice of palladium from the extended X-ray absorption fine structure (EXAFS) spectra [15, 20, 21] or X-ray diffraction [15, 20]. However, the above methods require, especially in the *in situ* mode, the use of a synchrotron radiation source, which is significantly more expensive compared with, for example, infrared (IR) spectroscopy.

Among the laboratory methods, Fourier-transform infrared spectroscopy (FTIR) is used to study the active sites of catalysts by means of probe molecules. This method is sensitive to the vibrations of molecules adsorbed on the catalyst surface [22]. Carbon monoxide (CO) is often used as a molecular probe, in which the vibrational frequency of the C–O bond depends on the charge state of the metal, the type of surface, and the adsorption geometry [20]. Nevertheless, in the available literature, no attempts have been made to distinguish *in situ*, based on FTIR data, the initial metal phase of palladium and hydrides and carbides coexisting and formed during the reaction. Since the charge state of palladium is known to affect the catalyst's activity [23], and different oxidation states (for example, Pd^0 and Pd^{2+}) can be easily distinguished from the vibrational frequency of adsorbed CO [24, 25], it is worth emphasizing that in the hydride and carbide phases, palladium remains in the Pd^0 state (only partial charge transfer, $|\delta| \ll 1$, takes place). It should also be noted that the use of CO as a probe molecule under the reaction conditions can affect the behavior of the material, since the presence of an additional reactive molecule and its adsorption on the active sites of the metal phase can affect the course of the catalytic reaction. In view of the latter, the use of

Abbreviations and notation: IR, infrared; FTIR, Fourier-transform IR spectroscopy; DRIFTS, diffuse reflectance infrared Fourier-transform spectroscopy; DFT, density functional theory; fcc, face-centered cubic (lattice); XPS, X-ray photoelectron spectroscopy; XANES, X-ray absorption near-edge structure; EXAFS, extended X-ray absorption fine structure.

intermediate reaction products formed during the catalytic process on the catalyst's surface as probe molecules looks very promising. For example, in the course of various hydrogenation/dehydrogenation reactions, the adsorption of hydrocarbons, which are good candidates for probe molecules, is expected on the palladium surface. While many works are devoted to the studying the evolution of hydrocarbons on the surface of noble metals [26–28], much less attention is paid to the study of phase transitions in palladium based on the analysis of the vibrational spectra of adsorbed hydrocarbons.

To develop a method for the quantitative description of the electronic subsystem of palladium using laboratory FTIR data, experimental measurements were carried out *in situ* using diffuse reflectance infrared Fourier-transform spectroscopy (DRIFTS) during the formation of hydride and carbide phases in palladium nanoparticles deposited on aluminum oxide under the influence of gas mixtures of carbon monoxide, hydrogen, and ethylene. The obtained experimental results were supported by calculations using the density functional theory method, reflecting the effect on the vibrational spectra of ethylidene adsorbed on the Pd(111) surface, the lattice parameters of fcc palladium, and the impurities of the palladium carbide phase.

MATERIALS AND METHODS

Materials, studied in this work, are palladium nanoparticles deposited on an aluminum oxide substrate (Pd/Al_2O_3). Samples were provided by Chimet S.p.A. (Arezzo, Italy) [29]. The mass content of palladium in the samples was 5%. The average size of nanoparticles, according to transmission electron microscopy, was 2.6 nm with a standard deviation of 0.4 nm [20, 21].

Experimental DRIFTS spectra were recorded on a Vertex 70 spectrometer (Bruker, Germany) with a cadmium mercury telluride detector. Measurements were performed with a resolution of 1 cm^{-1}, 64 scans per point, and automatically converted to absorption units by the Kubelka-Munk function. An original Python3 script was written to automatically normalize the spectra by area and subtract a spectrum of metal nanoparticles taken immediately after activation (*vide infra*). *In situ* data were obtained using the commercial *in situ* high temperature DRIFTS cell (Harrick Scientific Products Inc., USA) (see e.g., [20, 30]).

Sample activation was carried out in a hydrogen atmosphere at 125°C for a one hour. The sample was then cooled to the room temperature and kept in an inert medium. Under such conditions, the reference spectrum of the metal phase of palladium nanoparticles was recorded, which was subsequently used as a background. C_2H_4 was then sent through the sample while continuously recording IR spectra. The technique for obtaining experimental data and the experimental conditions are described in more detail in [20].

Experimental data in the presence of CO were obtained for a fresh sample after a similar activation procedure. In this case, the DRIFTS spectra of an activated sample cooled down to 30°C were recorded in H_2/He flow with the addition of 1% CO at various hydrogen concentrations.

Density functional theory (DFT) calculations were carried out within the generalized gradient approximation (GGA) [31] implemented in the VASP code [32, 33]. The Perdew–Burke-Ernzerhof (PBE) exchange-correlation functional [34, 35] was used together with the projector augmented wave method (PAW) applied to approximate 1*s* electrons of carbon and 1*s* to 4*p* electrons of palladium atoms. Brillouin zone was sampled using Monkhorst–Pack grid [36, 37], which makes it possible to choose the number of k-points k_1, k_2, k_3 in accordance with each $\mathbf{b}_i$ vector in the reciprocal space. A supercell of 45 palladium atoms was chosen, with five (111) layers of fcc palladium lattice. The cell was considered periodic along the x and y directions and had an additional 10 Å of vacuum along *the* z-axis to reconstruct the surface model. Although such a model of the Pd(111) surface did not reflect the real, more complex, surface structure of the nanoparticle, as shown below, it was sufficient to reproduce the experimental trends with moderate requirements for computing resources, corresponding to one adsorption site. In addition, it is also worth noting that other factors such as substrate, coverage, and temperature effects, which were not included in the model and discussed below, were not necessary to achieve the agreement between theoretical and experimental trends. A 9 × 9 × 1 grid of k-points and a cutoff energy of 500 eV (ENCUT parameter) were used based on the test calculations made to determine the dependence of the free energy on these parameters. To model the carbide impurities, carbon atoms were added to the centers of octahedral interstates in the fcc lattice of palladium. Ethylidene molecules ($C-CH_3$) were placed at the centers of triangles at (111) surface (*hollow* adsorption geometry). The vibrational frequencies were calculated using the Hessian matrix (the matrix of the second derivatives of the total energy with respect to the ion coordinates) using the density functional perturbation theory without symmetry restrictions. For each calculation, preliminary geometric relaxation was carried out by the conjugate gradient method [38, 39], and only the coordinates of atoms of adsorbed molecules were optimized, while the atoms of the palladium lattice and carbon atoms in the interstitial sites were fixed according to the known from the experimental data [40]. Cycles of optimization of the ionic and electronic subsystems (parameters EDIFFG and EDIFF) were carried out with convergence conditions of 10^{-5} and 10^{-6} eV, respectively.

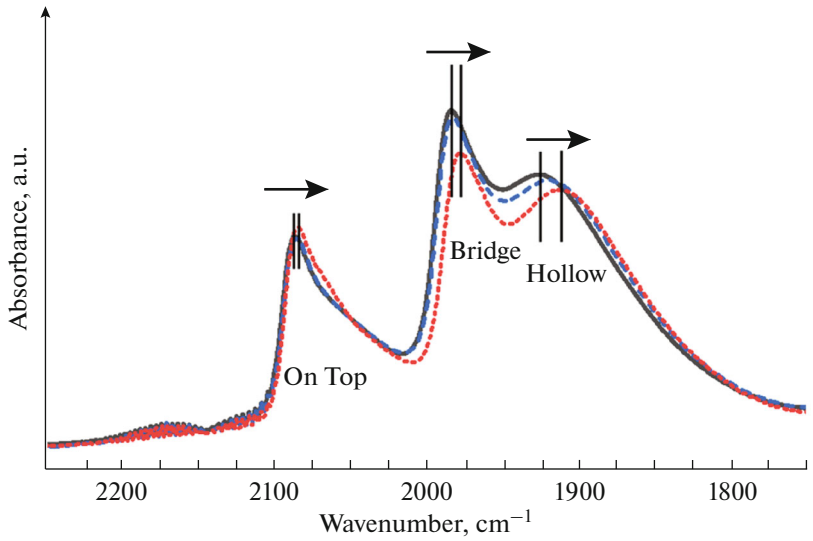

Fig. 1. Experimental DRIFTS spectra of a pre-activated Pd/Al_2O_3 sample in the range of C–O bond vibration, measured in the absence of hydrogen (solid black curve) and at hydrogen partial pressures of 20 (dashed blue) and 900 (red dots) mbar. The designations of peaks known from the literature are indicated and the shifts of their positions are highlighted.

RESULTS

The Effect of Palladium Hydride Formation on the Vibration Frequency of C–O Bond

CO is one of the most frequently used probe molecules for studying surfaces and active centers of catalysts by IR spectroscopy. In particular, it is possible to distinguish the types of surfaces and charge states of the metal, as well as the geometries of CO molecule adsorption based on the vibrational frequency of the C–O bond [27, 41–43]. In this section, we study a more subtle effect: the influence of hydrogen impurities in the palladium structure on the exact position of the vibrational frequency of the C–O bond of CO molecules adsorbed on the surface of palladium nanoparticles.

Palladium is known for its ability to absorb hydrogen, that dissociates on its surface, after which the formed atomic hydrogen predominantly occupies the octahedral interstitial sites of a fcc lattice of palladium. This effect is observed for both bulk and nanosized palladium samples [44, 45]. The hydride phase formed in palladium nanoparticles affects the catalytic properties of the material due to the changes in its electronic subsystem after the introduction of hydrogen [5, 9, 18, 46]. It is natural to expect that the fine structure of the DRIFTS spectra, in particular, the shape of the peaks and their exact positions, should also change.

Figure 1 shows a part of DRIFTS spectrum corresponding to the range of C–O bond stretch of a carbon monoxide molecule adsorbed on a palladium surface. The spectra were obtained at various partial pressures of hydrogen and a constant total pressure of the $CO/H_2/He$ gas mixture acting on the sample. The spectrum of the sample recorded immediately after Pd/Al_2O_3 activation was used as the subtracted background.

A simple comparison of the spectra indicates a change in the vibrational characteristics of adsorbed CO molecules upon formation of palladium hydride phase with respect to the initial metal phase. Out of the three peaks, associated with the three types of CO adsorption on the surface of palladium (*On Top*, *Bridge,* and *Hollow*, Figs. 2a–2c), *On Top* experience the least significant shift, while the other two are significantly red-shifted. On the other hand, the intensity of the *Bridge* and *Hollow peaks* noticeably falls, while that of *On Top* almost does not change.

The Influence of Palladium Carbide Formation on the Frequency of C–C Bonds

In a number of previous works, we reported the formation of palladium carbide in palladium nanoparticles even at close to the room temperatures due to interaction with the gas phase of acetylene [47, 48], ethylene [15, 20], and their mixtures with hydrogen [16, 49]. Upon adsorption of these hydrocarbons on palladium particles, formation of various carbon containing species and molecular fragments is possible [6, 20]. Based on the results gained from X-ray based bulk-sensitive techniques, that usually require the use of synchrotron radiation, palladium carbide was regarded as an interesting case for studying by DRIFTS methods in laboratory conditions. This motivated us to investigate the effect of carbide phase formation on the vibration frequencies of hydrocarbon molecules adsorbed on the palladium surface.

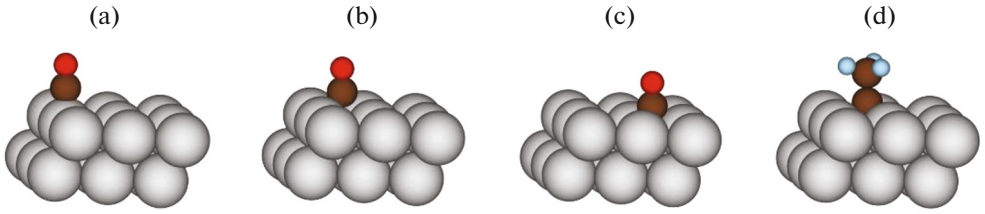

Fig. 2. Schematic representation of the adsorbed molecules considered: CO molecule in *On Top* (a), *Bridge* (b) and *Hollow* (c) configurations and an ethylidene molecule (d) adsorbed in the *Hollow* position.

We considered the adsorbed ethylidene (Fig. 2d), which can be formed on the catalyst upon exposure to ethylene (for example, in the reaction of ethylene hydrogenation). It should be noted that, unlike the case when carbon monoxide is added as a probe molecule, ethylidene is a natural part of a system. Ethylene, on the one hand, reacts with palladium nanoparticles to form an impurity carbide phase, and, on the other hand, forms intermediate structures on the catalyst surface, including ethylidene, which themselves can act as probe molecules. Figures 3 and 4 illustrate the effect of two factors considered in DFT simulation on the vibrational frequencies of the adsorbed molecules. The first one is associated with the lattice parameter of palladium, which changes due to the presence of the carbide phase [15, 20], to simulate the contribution of which a series of calculations were carried out with varying interplanar spacings along the (111) direction. Thus, the parameters of the triangle into whose center ethylidene is adsorbed (the adsorption geometry is *Hollow*) did not change. Nevertheless, a clear trend was observed in the vibrational frequencies of both C–C and C–H bonds, and in the "umbrella" mode of the methyl group, with the C–C bond length being roughly constant (Fig. 3).

At the next stage, the influence of the second factor was considered. Carbon atoms were placed in the octahedral interstitial sites of the fcc lattice without changing the lattice parameter. The positions of palladium atoms were not optimized both in the process of geometric optimization of adsorbed molecules and during the calculations of vibrational spectra. Obviously, the addition of even small impurities of carbon atoms leads to a strong shift in the characteristic vibrational frequencies of ethylidene molecules (Fig. 4), which is much larger than that observed for different lattice parameters.

The effect of carbon incorporation into the palladium lattice on the adsorption energy of ethylidene can be estimated from the difference between the energy of the system without adsorbed ethylidene and the energy of the complete system as a function of the number of incorporated carbon atoms (Fig. 5a). This strategy makes it possible to exclude the interaction energy of the intercalated carbon and palladium when considering the results of single-point calculations for these structures; however, the resulting energy is not the adsorption energy, since it includes the energy of adsorbed ethylidene. Thus, it is not the absolute values that matter, but the relative changes in energy as a function of the number of carbon atoms embedded in the palladium lattice. It can be concluded that the introduction of carbon makes the adsorption of ethylidene more energetically favorable, which coincides with the results of numerical DFT modeling of carbon monoxide adsorption using other models [50]. The influence of the change in the geometric characteristics of the considered supercell on the energy of the entire system suggests that, within the considered model, interatomic distances R_{Pd-Pd} are larger than in the crystal structure (Fig. 5b), which indicates the adequacy of the model and the correlation of the results with similar calculations using other functionals and structural models [25, 43, 51, 52].

To confirm the above theoretical results, an *in situ* DRIFTS experiment was carried out with a commercial Pd/Al_2O_3 catalyst. Continuous exposure to ethylene at room temperature resulted in a gradual transition from the original metal phase of the activated catalyst to the carbide phase. The spectrum of the activated sample taken before the catalyst was exposed to ethylene was used as a background. Figure 6 shows two regions of the DRIFTS spectrum after normalization and background subtraction. It is worth noting that data interpretation is hindered by (i) the strong contribution of the ethylene gas phase to the spectrum and (ii) the presence of many possible intermediate products formed in the process of ethylene adsorption on the palladium surface, the frequencies of which are especially overlapped in the region of C–H vibrations. In this case, the gas phase of ethylene dominates in the frequency range below 1100 cm^{-1}. In the range of 1400–1300 cm^{-1}, where the "umbrella" mode of the ethylidene methyl group is expected, the red-shift of the most intense peak is observed. The red-shift is in agreement with theoretical calculations, and the weakening of a peak with a lower frequency with an increase in the intensity of a new peak with a higher wave number is in agreement with the well-known property of palladium to exist in different phases with different lattice parameters at different concentrations of impurities. This behavior has been studied espe-

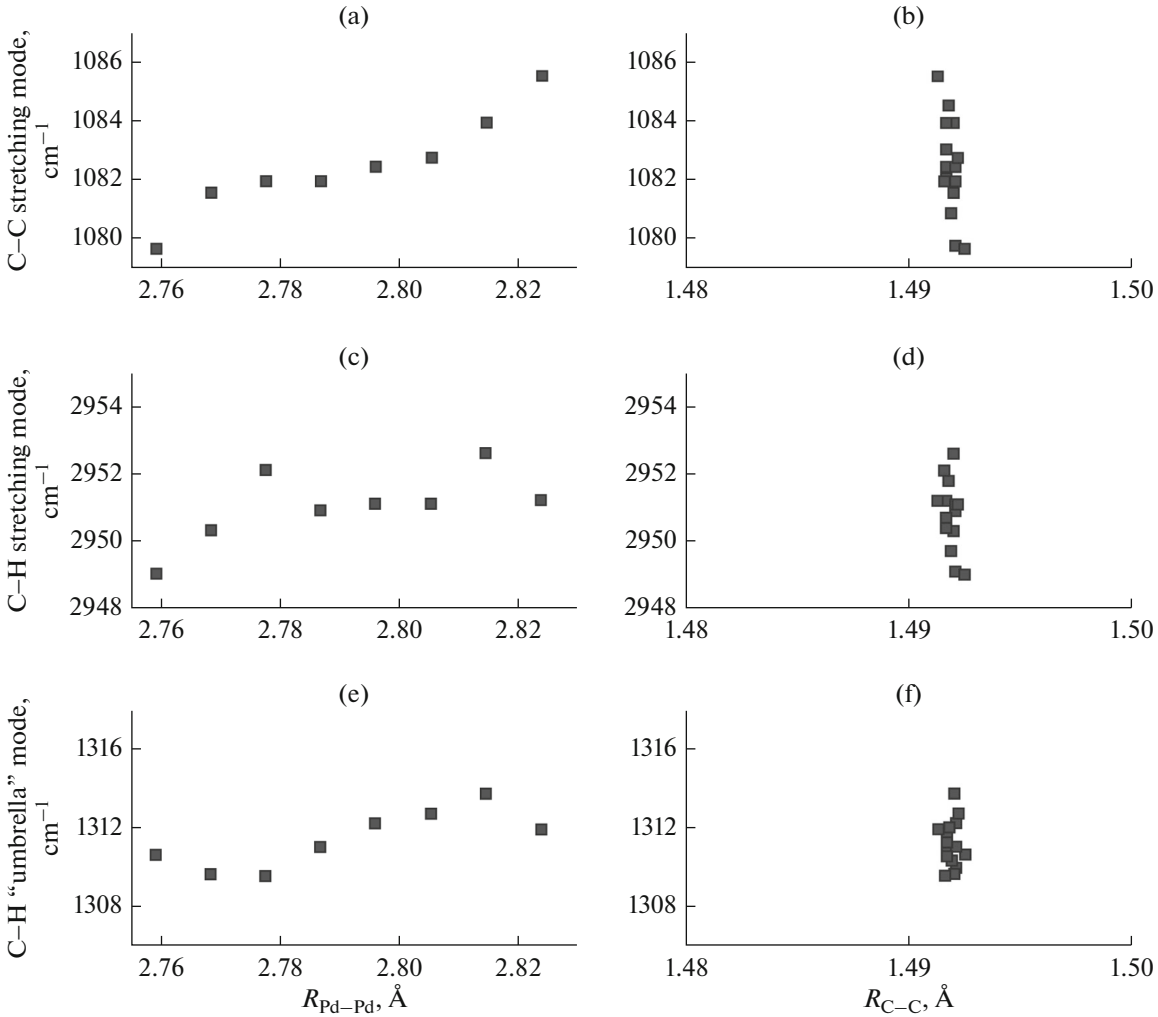

Fig. 3. Positions of vibrational frequencies of (a, b) C–C and (c, d) C–H bonds stretch and (e, f) C–H "umbrella" mode depending on the Pd–Pd interatomic distances between the nearest Pd atoms in the surface and the first near-surface layers (a, c, e) and on the C–C bond length (b, d, f) in the ethylidene molecule.

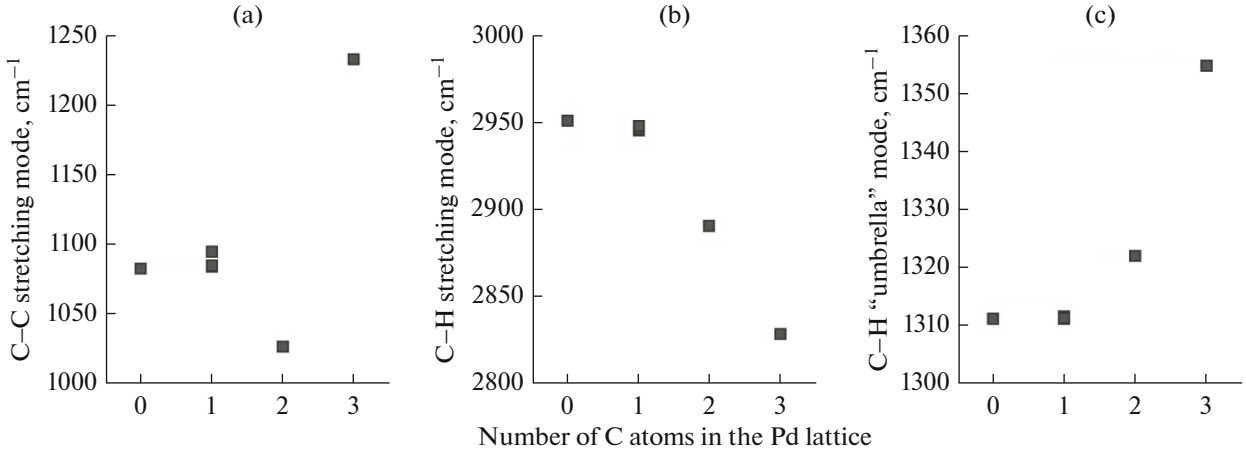

Fig. 4. Positions of the vibrational frequencies of the C–C (a), C–H (b) bond stretches and the "umbrella" C–H mode of the methyl group of ethylidene (c) depending on the number of carbon atoms in the interstitial sites of palladium close to the adsorbed ethylidene molecule.

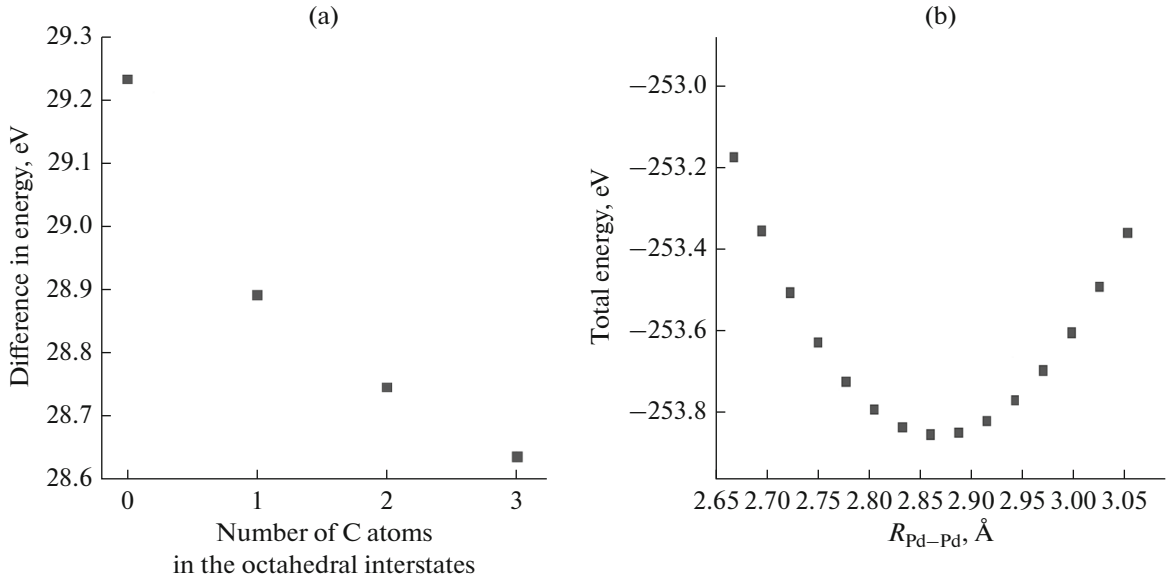

Fig. 5. Energy difference between the structure without ethylidene and the energy of the complete structure as function of the number of carbon atoms embedded in the octahedral interstitials of the fcc lattice of palladium (a); and (b) total energy of the system without interstitial carbon atoms as a function of interatomic distances R_{Pd-Pd}.

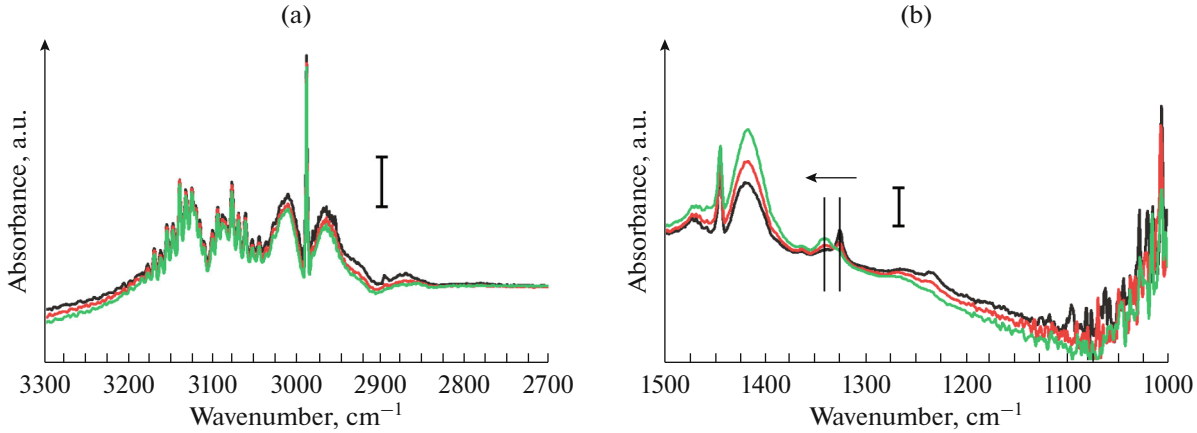

Fig. 6. Background subtracted experimental DRIFTS spectra in the region of C–H (a) and C–C (b) vibrations, measured after 5 (black), 10 (red), and 30 (green) minutes of exposure to ethylene flow of the activated Pd/Al_2O_3 catalyst.

cially well for palladium hydrides, but carbide structures also exhibit similar properties [46].

It should be noted that the formation of the carbide phase of palladium under the action of ethylene on the catalyst may be accompanied by the formation of the hydride phase. Nevertheless, the available literature data suggests that the former is dominant, and the theoretical calculations performed earlier allow us to expect the addition of the two contributions to the experimentally observed red-shift [15, 20].

Comparison of the absolute values of the frequencies obtained from DFT simulations and those determined experimentally, indicates a discrepancy between the initial positions of the peaks, which can reach 50 cm^{-1} [20, 25]. This can be due to the neglecting of the influence of the substrate and the adsorbate-adsorbate interaction as a function of the coverage [43, 51]. The adequacy of choice of the functional for describing such an interaction [52] should be noted, as well as the correlation of the obtained results with the calculations, where the nanoparticle model is a cluster [25, 43], and also that the structural model discussed in this paper contains periodic boundary conditions along the *x* and *y axes* and, accordingly, includes interactions of adsorbates at positions equivalent with respect to translations along *x* and *y* (in contrast to

cluster models), corresponding to a low coverage. Thus, the calculation model used is simplified, but sufficient to reproduce the observed experimental trends.

DISCUSSION

Expanding the capabilities of vibrational spectroscopy is of considerable interest, especially in the field of developing quantitative approaches for *in situ* characterization of catalysts. Most of the studies are devoted to the search for relationships between the IR spectra of adsorbed CO molecules and the structural parameters of noble metal nanoparticles. Thus, in [53] an analysis of the morphology of the surface of a platinum catalyst was carried out using IR spectra, and in [54] the correlation between the vibrational frequencies of CO and the coordination numbers of Pt active sites was considered. In the present work, we explore the possibility to characterize the electronic structure of supported palladium catalysts.

As shown by the example of the shift in the vibrational frequency of the C–O bond during CO adsorption on the surface of pure metal particles and palladium hydride, DRIFTS spectroscopy can provide information on minor changes in the electronic substructure of palladium during the formation of the hydride phase. It is known that hydrogen in the palladium lattice is in an ionized state [55], which is consistent with the observed red shift in the frequency of C-O vibrations of carbon monoxide.

The second example demonstrates an interesting case of time evolution of the vibrational properties of one of the intermediates of the reaction, which, in turn, can be used to describe the evolution of the catalyst's structure without adding a probe molecule to the system. It should be noted that, in both the metal and carbide phases, palladium atoms remain in the Pd^0 state, and the maximum C : Pd ratio does not rise above 0.13 even at higher temperatures [21]. Therefore, it is much more difficult to detect such small changes than to distinguish, for example, between Pd^{2+} and Pd^0 using probe molecules. In this regard, other methods sensitive to the palladium carbide phase deserve mention. In particular, in a number of works, one can find cases of using XPS to determine the PdC phase in a palladium catalyst under the influence of hydrocarbons [4, 9, 18, 56]. The incorporation of carbon into the subsurface layers of palladium leads to the appearance of an additional peak in the Pd $3d_{5/2}$ spectrum, which is higher by 0.6 eV relative to the peak of the metal phase. Although much progress has been made in the field of *in situ* XPS application at pressures up to tens of mbar [57], this method is still not widely used. It is also known that Pd *K*-edge EXAFS and XANES spectra can distinguish between hydride and carbide phases of the Pd^0 catalyst [15, 20, 21]. However, the tiny spectral changes require the use of first-principles modeling or machine learning methods to extract information about the states of PdC and PdH [58–61]. Significantly more information could be provided by similar measurements of the *L*- and *M*-edges of Pd, as well as the Fourier analysis of EXAFS up to the third coordination shell, but in the first case, the experiment is complicated by utilization of soft X-ray radiation. Like XANES and XPS, the DRIFTS spectra are sensitive to the evolution of the electronic subsystem of palladium, which makes it possible to study the relationship between small shifts in the vibrational frequencies of adsorbates and the structural parameters of nanoparticles. However, we did not find any reports of such influence of the formation of carbide or hydride phases on the shift of vibrational modes.

The results presented in this work allow us to speak about the relationship between the structural parameters of palladium nanoparticles, which undergo changes due to the formation of new phases, and the fine structure of the vibrational spectra of adsorbed molecules. Therefore, vibrational spectroscopies that are sensitive to probe molecules or even intermediates, such as the FTIR, can act as *in situ* methods for characterization of the electronic structure of catalysts under reaction conditions when it is difficult to use other methods that are more difficult to implement. It should be noted that in the context of the considered FTIR, we are talking about the use of the latter as a quantitative, and not just a qualitative tool, as opposed to the traditional approach based on the "fingerprint" method. It is extremely important to use the vibrational modes of one of the compounds adsorbed in the course of the reaction as a probe of the electronic structure, which makes it possible to exclude the addition of probe molecules that can affect the ongoing processes.

Based on the experimental and theoretical results obtained in this work, we can conclude that the extraction of quantitative data from IR spectra, such as the concentration of a carbide impurity in palladium, is potentially possible, however, it is complicated by many factors, among which should be mentioned temperature effects, competitive adsorption, coverage effects and many more. Thus, it is necessary to carry out experimental studies of well-known systems under model conditions in order to reveal more accurate dependences of the structure–spectrum type.

CONCLUSION

We have found the influence of carbide and hydride impurities in the bulk of the palladium lattice on the vibrational modes corresponding to hydrocarbon and CO molecules adsorbed on its surface. This was established by theoretical DFT calculations and confirmed by DRIFTS experiments. Based on the conducted research, the following important conclusions can be drawn:

(1) small changes in peak positions in vibrational spectra can and should be analyzed to obtain additional information about the atomic and electronic structure of the catalyst;

(2) reactants are able to act as probe molecules by themselves.

The found dependencies serve as the basis for a quantitative approach to the analysis of IR spectra, which opens new possibilities for monitoring the formation of palladium carbides and hydrides in the course of reactions.

FUNDING

The study was carried out with the financial support of the Russian Ministry of Education and Science (Agreement no. 075-15-2021-1389 dated October 13, 2021).

CONFLICT OF INTERESTS

The authors declare no conflict of interest requiring disclosure in this article.

REFERENCES

1. Bond, G., Dowden, D., and Mackenzie, N., The selective hydrogenation of acetylene, *Trans. Faraday Soc.*, 1958, vol. 54, p. 1537.
2. Borodziński, A. and Bond, G.C. Selective hydrogenation of ethyne in ethene-rich streams on palladium catalysts, Part 2: Steady-state kinetics and effects of palladium particle size, carbon monoxide, and promoters, *Catal. Rev.*, 2008, vol. 50, no. 3, p. 379.
3. Teschner, D., Borsodi, J., Kis, Z., Szentmiklosi, L., Revay, Z., Knop-Gericke, A., Schlogl, R., Torres, D., and Sautet, P., Role of Hydrogen Species in Palladium-Catalyzed Alkyne Hydrogenation, *J. Phys. Chem. C,* 2010, vol. 114, no. 5, p. 2293.
4. Teschner, D., Borsodi, J., Wootsch, A., Revay, Z., Havecker, M., Knop-Gericke, A., Jackson, S.D., and Schlögl, R., The roles of subsurface carbonband hydrogen in palladium-catalyzed alkyne hydrogenation, *Science*, 2008, vol. 320, no. 5872, p. 86.
5. Borodziński, A.and Bond, G.C. Selective hydrogenation of ethyne in ethene-rich streams on palladium catalysts. Part 1. Effect of changes to the catalyst during reaction, *Catal. Rev.*, 2006, vol. 48, no. 2, p. 91.
6. Molnár, Á., Sárkány, A., and Varga, M. Hydrogenation of carbon–carbon multiple bonds: chemo-, regio- and stereo-selectivity, *J. Mol. Catal. A: Chem.*, 2001, vol. 173, no. 1, p. 185.
7. Stahl, S.S., Palladium oxidase catalysis: selective oxidation of organic chemicals by direct dioxygen-coupled turnover, *Angew. Chem., Int. Ed.*, 2004, vol. 43, no. 26, p. 3400.
8. Groppo, E., Lazzarini, A., Carosso, M., Bugaev, A., Manzoli, M., Pellegrini, R., Lamberti, C., Banerjee, D., and Longo, A., Dynamic behavior of Pd/P4VP catalyst during the aerobic oxidation of 2-propanol: A simultaneous SAXS/XAS/MS operando study, *ACS Catal.,* 2018, vol. 8. C. 6870.
9. Armbrüster, M., Behrens, M., Cinquini, F., Föttinger, K., G Grin, Y., Haghofer, A., Klotzer, B., Knop-Gericke, A., Lorenz, H., Ota, A., Penner, S., Prinz, J., Rameshan, C., Revay, Z., Rosenthal, D., et al., How to control the selectivity of palladium-based catalysts in hydrogenation reactions: The Role of subsurface chemistry, *ChemCatChem*, 2012, vol. 4, no. 8, p. 1048.
10. Ma, H., Chen, M., Sun, L., Feng, H., Zhan, X., and Xie, Y., *Kinet. Catal.*, 2021, vol. 62, no. 6, p. 750.
11. Burch, R. and Loader, P.K., Investigation of Pt/Al_2O_3 and Pd/Al_2O_3 catalysts for the combustion of methane at low concentrations, *Appl. Catal., B,* 1994, vol. 5, nos. 1–2, p. 149–164.
12. Losch, P., Huang, W., Vozniuk, O., Goodman, E.D., Schmidt, W., and Cargnello, M., Modular Pd/Zeolite composites demonstrating the key role of support hydrophobic/hydrophilic character in methane catalytic combustion, *ACS Catal.,* 2019, vol. 9, no. 6, p. 4742.
13. Ma, J., Lou, Y., Cai, Y., Zhao, Z., Wang, L., Zhan, W., Guo, Y., and Guo, Y., The relationship between the chemical state of Pd species and the catalytic activity for methane combustion on Pd/CeO_2, *Catal. Sci. Technol.*, 2018, vol. 8, no. 10, p. 2567 .
14. Padilla, J.M., Del Angel, G., and Navarrete, J., Improved $Pd/\gamma\text{-}Al_2O_3$–Ce catalysts for benzene combustion, *Catal. Today,* 2008, vols. 133–135, p. 541.
15. Skorynina, A.A., Tereshchenko, A.A., Usoltsev, O.A., Bugaev, A.L., Lomachenko, K.A., Guda, A.A., Groppo, E., Pellegrini, R., Lamberti, C., and Soldatov, A.V., Time-dependent carbide phase formation in palladium nanoparticles, *Radiat. Phys. Chem.*, 2020, vol. 175, p. 108079.
16. Bugaev, A.L., Guda, A.A., Pankin, I.A., Groppo, E., Pellegrini, R., Longo, A., Soldatov, A.V., and Lamberti, C., The role of palladium carbides in the catalytic hydrogenation of ethylene over supported palladium nanoparticles, *Catal. Today,* 2019, vol. 336, p. 40.
17. Bugaev, A.L., Zabilskiy, M., Skorynina, A.A., Usoltsev, O.A., Soldatov, A.V., and van Bokhoven, J.A., In situ formation of surface and bulk oxides in small palladium nanoparticles, *Chem. Commun.,* 2020, vol. 56, no. 86, p. 13097.
18. Bennett, P.A. and Fuggle, J.C., Electronic structure and surface kinetics of palladium hydride studied with x-ray photoelectron spectroscopy and electron-energy-loss spectroscopy, *Phys. Rev. B,* 1982, vol. 26, no. 11, p. 6030.
19. Guda, A.A., Guda, S.A., Lomachenko, K.A., Soldatov, M.A., Pankin, I.A., Soldatov, A.V., Braglia, L., Bugaev, A.L., Martini, A., Signorile, M., Groppo, E., Piovano, A., Borfecchia, E., and Lamberti, C., Quantitative structural determination of active sites from in situ and operando XANES spectra: From standard ab initio simulations to chemometric and machine learning approaches, *Catal. Today,* 2019, vol. 336, p. 3.
20. Usoltsev, O.A., Pnevskaya, A.Y., Kamyshova, E.G., Tereshchenko, A.A., Skorynina, A.A., Zhang, W., Yao, T., Bugaev, A.L., and Soldatov, A.V., Dehydrogenation of ethylene on supported palladium nanoparticles: A double view from metal and hydrocarbon sides, *Nanomaterials*, 2020, vol. 10, no. 9, p. 1643.

21. Bugaev, A.L., Guda, A.A., Lazzarini, A., Lomachenko, K.A., Groppo, E., Pellegrini, R., Piovano, A., Emerich, H., Soldatov, A.V., Bugaev, L.A., Dmitriev, V.P., van Bokhoven, J.A., and Lamberti, C., In situ formation of hydrides and carbides in palladium catalyst: when XANES is better than EXAFS and XRD, *Catal. Today*, 2017, vol. 283, p. 119.

22. Avery, N.R., Infrared spectra of olefins adsorbed on silica supported palladium, *J. Catal.*, 1970, vol. 19, no. 1, p. 15.

23. Ustyugov, A.V., Korypaeva, V.V., Obeidat, Z.Z., Putin, A.Yu., Shvarts, A.L., and Bruk, L.G., *Kinet. Catal.*, 2022, vol. 63, no. 2, p. 226.

24. Zhang, Y., Cai, Y., Guo, Y., Wang, H., Wang, L., Lou, Y., Guo, Y., Lu, G., and Wang, Y., The effects of the Pd chemical state on the activity of Pd/Al_2O_3 catalysts in CO oxidation, *Catal. Sci. Technol.*, 2014, vol. 4, no. 11, p. 3973.

25. Aleksandrov, H.A., Neyman, K.M., Hadjiivanov, K.I., and Vayssilov, G.N., Can the state of platinum species be unambiguously determined by the stretching frequency of an adsorbed CO probe molecule?, *Phys. Chem. Chem. Phys.*, 2016, vol. 18, no. 32, p. 22108.

26. Tillekaratne, A., Simonovis, J.P., and Zaera, F., Ethylene hydrogenation catalysis on Pt(111) single-crystal surfaces studied by using mass spectrometry and in situ infrared absorption spectroscopy, *Surf. Sci.*, 2016, vol. 652, p. 134.

27. Zaera, F., New advances in the use of infrared absorption spectroscopy for the characterization of heterogeneous catalytic reactions, *Chem. Soc. Rev.*, 2014, vol. 43, no. 22, p. 7624.

28. Zaera, F., Janssens, T.V.W., and Öfner, H., Reflection absorption infrared spectroscopy and kinetic studies of the reactivity of ethylene on Pt(111) surfaces, *Surf. Sci.*, 1996, vol. 368, nos. 1–3, p. 371.

29. Agostini, G., Groppo, E., Piovano, A., Pellegrini, R., Leofanti, G., and Lamberti, C., Preparation of supported Pd catalysts: from the Pd precursor solution to the deposited Pd^{2+} phase, *Langmuir*, 2010, vol. 26, no. 13, p. 11204.

30. Pnevskaya, A.Y., Bugaev, A.L., Tereshchenko, A.A., and Soldatov, A.V., Experimental and theoretical investigation of ethylene and 1-MCP binding sites in HKUST-1 metal-organic framework, *J. Phys. Chem. C,* 2021, vol. 125, no. 40, p. 22295.

31. Perdew, J.P., Accurate density functional for the energy: Real-space cutoff of the gradient expansion for the exchange hole, *Phys. Rev. Lett.*, 1985, vol. 55, no. 16, p. 1665.

32. Kresse, G. and Furthmüller, J., Efficincy of ab-initio total energy calculations for metals and semiconductors using a plane-wave basis set, *Comput. Mater. Sci.*, 1996, vol. 6, p. 15.

33. Kresse, G. and Furthmüller, J., Efficient iterative schemes for ab initio total-energy calculations using a plane-wave basis set, *Phys. Rev. B,* 1996, vol. 54, no. 16, p. 11169.

34. Paier, J., Hirschl, R., Marsman, M., and Kresse, G., The Perdew-Burke-Ernzerhof exchange-correlation functional applied to the G2-1 test set using a plane-wave basis set, *J. Chem. Phys.,* 2005, vol. 122, no. 23, p. 234102.

35. Paier, J., Marsman, M., Hummer, K., Kresse, G., Gerber, I.C., and Angyan, J.G., Screened hybrid density functionals applied to solids, *J. Chem. Phys.,* 2006, vol. 124, no. 15, p. 154709.

36. Evarestov, R.A. and Smirnov, V.P., Modification of the Monkhorst-Pack special points meshes in the Brillouin zone for density functional theory and Hartree–Fock calculations, *Phys. Rev. B,* 2004, vol. 70, no. 23, p. 233101.

37. Pack, J.D. and Monkhorst, H.J., Special points for Brillouin-zone integrations, *Phys. Rev. B,* 1977, vol. 16, no. 4, p. 1748.

38. Shewchuk, J.R., An introduction to the conjugate gradient method without the agonizing pain, in *An introduction to the conjugate gradient method without the agonizing pain*, Carnegie Mellon University, 1994.

39. Steihaug, T., The conjugate gradient method and trust regions in large scale optimization, *SIAM J. Numer. Anal.*, 1983, vol. 20, no. 3, p. 626.

40. Bugaev, A.L., Usoltsev, O.A., Guda, A.A., Lomachenko, K.A., Pankin, I.A., Rusalev, Y.V., Emerich, H., Groppo, E., Pellegrini, R., Soldatov, A.V., van Bokhoven, J.A., and Lamberti, C., Palladium carbide and hydride formation in the bulk and at the surface of palladium nanoparticles, *J. Phys. Chem. C,* 2018, vol. 122, no. 22, p. 12029.

41. Szanyi, J., Kuhn, W., and Goodman, D., CO adsorption on Pd(111) and Pd(100): Low and high pressure correlations, *J. Vac. Sci. Technol. A,* 1993, vol. 11, p. 1969.

42. Tereshchenko, A., Guda, A., Polyakov, V., Rusalev, Y., Butova, V., and Soldatov, A., Pd nanoparticle growth monitored by DRIFT spectroscopy of adsorbed CO, *Analyst*, 2020, vol. 145, no. 23, p. 7534.

43. Zeinalipour-Yazdi, C.D., Willock, D.J., Thomas, L., Wilson, K., and Lee, A.F., CO adsorption over Pd nanoparticles: A general framework for IR simulations on nanoparticles, *Surf. Sci.*, 2016, vol. 646, p. 210.

44. Bugaev, A.L., Guda, A.A., Lomachenko, K.A., Shapovalov, V.V., Lazzarini, A., Vitillo, J.G., Bugaev, L.A., Groppo, E., Pellegrini, R., Soldatov, A.V., van Bokhoven, J.A., and Lamberti, C., Core–Shell structure of palladium hydride nanoparticles revealed by combined X-ray absorption spectroscopy and X-ray diffraction, *J. Phys. Chem. C,* 2017, vol. 121, no. 33, p. 18202.

45. Setayandeh, S.S., Gould, T., Vaez, A., McLennan, K., Armanet, N., and Gray, E., First-principles study of the atomic volume of hydrogen in palladium, *J. Alloys Compd.*, 2021, vol. 864, p. 158713.

46. Bugaev, A.L., Usoltsev, O.A., Guda, A.A., Lomachenko, K.A., Brunelli, M., Groppo, E., Pellegrini, R., Soldatov, A.V., and van Bokhoven, J., Hydrogenation of ethylene over palladium: Evolution of the catalyst structure by operando synchrotron-based techniques, *Faraday Discuss.,* 2021, vol. 229, p. 197.

47. Bugaev, A.L., Usoltsev, O.A., Lazzarini, A., Lomachenko, K.A., Guda, A.A., Pellegrini, R., Carosso, M., Vitillo, J.G., Groppo, E., van Bokhoven, J.A., Soldatov, A.V., and Lamberti, C., Time-resolved operando studies of carbon supported Pd nanoparticles under hy-

drogenation reactions by X-ray diffraction and absorption, *Faraday Discuss.*, 2018, vol. 208, p. 187.

48. Bugaev, A.L., Guda, A.A., Lomachenko, K.A., Kamyshova, E.G., Soldatov, M.A., Kaur, G., Øien-Ødegaard, S., Braglia, L., Lazzarini, A., Manzoli, M., Bordiga, S., Olsbye, U., Lillerud, K.P., Soldatov, A.V., and Lamberti, C., Operando study of palladium nanoparticles inside UiO-67 MOF for catalytic hydrogenation of hydrocarbons, *Faraday Discuss.*, 2018, vol. 208, p. 287.
49. Bugaev, A.L., Guda, A.A., Pankin, I.A., Groppo, E., Pellegrini, R., Longo, A., Soldatov, A.V., and Lamberti, C., Operando X-ray absorption spectra and mass spectrometry data during hydrogenation of ethylene over palladium nanoparticles, *Data Brief.*, 2019, vol. 24, p. 103954.
50. Yudanov, I.V., Neyman, K.M., and Rösch, N., Density functional study of Pd nanoparticles with subsurface impurities of light element atoms, *Phys. Chem. Chem. Phys.,* 2004, vol. 6, no. 1, p. 116.
51. Mason, S.E., Grinberg, I., and Rappe, A.M., Adsorbate–adsorbate interactions and chemisorption at different coverages studied by accurate ab initio calculations: CO on Transition metal surfaces, *J. Phys. Chem. B*, 2006, vol. 110, no. 8, p. 3816.
52. Tereshchenko, A., Pashkov, D., Guda, A., Guda, S., Rusalev, Y., and Soldatov, A., Adsorption sites on Pd Nanoparticles unraveled by machine-learning potential with adaptive sampling, *Molecules*, 2022, vol. 27, no. 2, p. 357.
53. Lansford, J.L. and Vlachos, D.G., Infrared spectroscopy data- and physics-driven machine learning for characterizing surface microstructure of complex materials, Nat. Commun., 2020, vol. 11, no. 1, p. 1513.
54. Kappers, M.J. and van der Maas, J.H., Correlation between CO frequency and Pt coordination number. A DRIFT study on supported Pt catalysts, *Catal. Lett.,* 1991, vol. 10, no. 5, p. 365.
55. Koroteev, Yu.M., Gimranova, O.V., and Chernov, I.P., Phys. Solid Stat, 2011, vol. 53, no. 5, p. 896.
56. Teschner, D., Revay, Z., Borsodi, J., Havecker, M., Knop-Gericke, A., Schlogl, R., Milroy, D., Jackson, S.D., Torres, D., and Sautet, P., Understanding palladium hydrogenation catalysts: when the nature of the reactive molecule controls the nature of the catalyst active phase, *Angew. Chem., Int. Ed.*, 2008, vol. 47, no. 48, p. 9274.
57. Lee, A.F., Naughton, J.N., Liu, Z., and Wilson, K., High-pressure XPS of crotyl alcohol selective oxidation over metallic and oxidized Pd(111), *ACS Catal.,* 2012, vol. 2, no. 11, p. 2235.
58. Usoltsev, O.A., Bugaev, A.L., Guda, A.A., Guda, S.A., and Soldatov, A.V., How much structural information could be extracted from XANES spectra for palladium hydride and carbide nanoparticles, *J. Phys. Chem. C,* 2022.
https://doi.org/10.1021/acs.jpcc.1c09420
59. Meza, RamirezC.A., Greenop, M., Ashton, L., and Rehman, I.U., Applications of machine learning in spectroscopy, *Appl. Spectrosc. Rev.*, 2021, vol. 56, nos. 8–10, p. 733.
60. Guda, A.A., Guda, S.A., Martini, A., Kravtsova, A.N., Algasov, A., Bugaev, A., Kubrin, S.P., Guda, L.V., Šot, P., van Bokhoven, J.A., Copéret, C., and Soldatov, A.V., Understanding X-ray absorption spectra by means of descriptors and machine learning algorithms, *NPJ Comput. Mater.*, 2021, vol. 7, no. 1, p. 203.
61. Martini, A., Guda, S.A., Guda, A.A., Smolentsev, G., Algasov, A., Usoltsev, O., Soldatov, M.A., Bugaev, A., Rusalev, Y., Lamberti, C., and Soldatov, A.V., PyFitit: The software for quantitative analysis of XANES spectra using machine-learning algorithms, *Comput. Phys. Commun.*, 2020, vol. 250, p. 107064.